Carbohydrate Polymers 93 (2013) 401–411

Contents lists available at SciVerse ScienceDirect

Carbohydrate Polymers

journal homepage: www.elsevier.com/locate/carbpol

Effects of Ar–H_2–N_2 microwave plasma on chitosan and its nanoliposomes blend thin films designed for tissue engineering applications

H.Y. Zhang[a,b], F. Cleymand[a,b,*], C. Noël[a,b], C.J.F. Kahn[c,d,e], M. Linder[f], A. Dahoun[a,b], G. Henrion[a,b], E. Arab-Tehrany[f]

[a] CNRS, Institut Jean Lamour, UMR 7198, F-54042 Nancy, France
[b] Université de Lorraine, Institut Jean Lamour UMR 7198 CNRS, Ecole des Mines, Parc de Saurupt, CS 14234, 54042 Nancy, France
[c] Aix-Marseille Université, LBA UMRT 24, Marseille, France
[d] Faculté de Médecine Secteur Nord, Boulevard P. Dramard, 13916 Marseille, France
[e] IFSTTAR, LBA UMRT 24, Marseille, France
[f] Université de Lorraine, Laboratoire d'Ingénierie des Biomolécules, 2, Avenue de la Forêt de Haye, F-54504 Vandœuvre-Lès-Nancy Cedex, France

ARTICLE INFO

Article history:
Received 25 September 2012
Received in revised form 5 December 2012
Accepted 7 December 2012
Available online 19 December 2012

Keywords:
Chitosan
Nanoliposome
Lecithin
Plasma treatment
Doehlert experimental design
Functionalization

ABSTRACT

This work addresses the functionalization of chitosan thin films and its nanoliposomes blend films by a microwave-excited $Ar/N_2/H_2$ surface-wave plasma treatment which was found an effective tool to modify surface properties. Changes in the film properties (wettability, chemical composition, morphology) induced by the plasma treatment are studied using water contact angle measurements, X-ray photoelectron spectroscopy and scanning probe microscopy. The results suggest that hydrophilicity of the films is improved by plasma treatment in a plasma condition dependency manner. Water contact angle of chitosan films before and after plasma treatment are, respectively, 101° and 27°. Besides chemical changes on the surface, the nanoliposomes incorporation and plasma treatment also induce morphological modifications. Moreover, a correlation is found between the nanoliposomes composition and size, and the effects of plasma treatment. It is shown that the plasma treatment significantly improves the chitosan film functionalization. The effect of N_2 content (88% and 100%) in the plasma gas mixture on the film etching is also pointed out.

1. Introduction

As a biomaterial that exhibits an excellent biocompatibility and admirable biodegradability, chitosan has been largely used in the field of tissue engineering, drug delivery, and gene therapy (Bhardwaj & Kundu, 2011; Casettari et al., 2012; Dash, Chiellini, Ottenbrite, & Chiellini, 2011; Domard, 2011; Duarte, Mano, & Reis, 2010; Hoemann, Sun, Légaré, McKee, & Buschmann, 2005; Ji, Annabi, Khademhosseini, & Dehghani, 2011; Muzzarelli, Greco, Busilacchi, Sollazzo, & Gigante, 2012; Prabaharan & Jayakumar, 2009). Nevertheless, chitosan films suffer from low wetting properties in aqueous basic media with pH value higher than 7. This represents a drawback for the production of scaffolds for tissue engineering application.

Previous works show that by adding natural nanoliposomes based on vegetable and marine lecithin, the surface wettability of chitosan and blend films increased because nanoliposomes present polar phospholipids (Zhang et al., 2012). The choice of nanoliposomes has been preferred to liposome because of their higher surface contact area and their potential ability to increase solubility and to enhance bioavailability of the encapsulated material to a greater extent (Mozafari, 2005). The main constituents of nanoliposomes are phospholipids, which are amphiphilic molecules containing a water-soluble hydrophilic head section and a lipid-soluble hydrophobic tail section (Nirmala et al., 2011). The nanoliposomes in this work were prepared based on soya, rapeseed and marine lecithins. Rapeseed and soya lecithins consist mainly of three mono- and poly-unsaturated fatty acids namely oleic (C18:1), linoleic (C18:2), and linolenic acids (C18:3). Linoleic and linolenic acids are considered essential fatty acids because they are important to human health and our body cannot synthesize them (Coonrod, Brick, Byrne, DeBonte, & Chen, 2008). Marine lecithin from salmon (*Salmo salar*) contains a high percentage of polyunsaturated fatty acids (PUFAs), especially eicosapentaenoic acid (EPA, 20:5n-3) and docosahexaenoic acid (DHA, 22:6n-3) (Belhaj,

* Corresponding author at: CNRS, Institut Jean Lamour, UMR 7198, F-54042 Nancy, France. Tel.: +33 3 83 58 42 59; fax: +33 3 83 53 47 64.
E-mail addresses: zhang_hong_yuan@hotmail.com (H.Y. Zhang), franck.cleymand@ijl.nancy-universite.fr (F. Cleymand).

0144-8617/$ – see front matter © 2012 Elsevier Ltd. All rights reserved.
http://dx.doi.org/10.1016/j.carbpol.2012.12.015

Arab-Tehrany, & Linder, 2010). Numerous studies, both in humans and in animals, have demonstrated that PUFAs of the n-3 series, especially EPA and DHA, are necessary to several physiological processes (Mirajkar, Jamadar, Patil, & Mirajkar, 2011).

Plasma processes which are well-known tools to modify the properties of polymer surfaces (Belmonte et al., 2005; Hody, Belmonte, Czerwiec, Henrion, & Thiebaut, 2006; Hody, Belmonte, Pintassilgo, et al., 2006; Moser, Gilliéron, & Henrion, 2010; Ogino, Kral, Yamashita, & Nagatsu, 2008; Wanichapichart, Sungkum, Taweepreda, & Nisoa, 2009). This process could increase the wettability of chitosan films resulting in an improvement of the cell adhesion on chitosan surface (Morra, Occhiello, & Garbassi, 1989). The most critical parameters of the plasma treatment are the injected power, gas mixture composition, and process duration. In the present study, $Ar/N_2/H_2$ gas mixture was used, because such a plasma atmosphere is considered to be an effective precursor to introduce amine functional groups onto the material, thus enhancing their hydrophilicity and surface energy (Chen et al., 2010; Inagaki, Narushima, Hashimoto, & Tamura, 2007; Kral, Ogino, & Nagatsu, 2008). Doehlert experimental design was used to obtain a number of distinct levels and the response surface methodology (RSM) was applied as an effective tool to get an optimal response.

The aim of this work is to functionalize chitosan films and its nanoliposomes blend matrix surface by cold plasma treatment for tissue engineering applications. In the first time, we characterized the fatty acid composition, lipid class, size and electrophoretic mobility of nanoliposomes. Then, several surface properties of films before and after cold plasma treatment were analyzed such as morphology and roughness, elemental composition and chemical bonds, water contact angle, and surface energy (Digidrop).

2. Experimental details

2.1. Chemical product details

Chitosan samples were prepared from shrimp shells, practical grade. Their deacetylation degree was higher than 75% (Sigma–Aldrich, molecular weight 50–190 kDa, DD ≥ 75%, viscosity 200–2000 mPa s). The fish lecithin were extracted from *S. salar*, rapeseed and soya lecithins were produced by enzymatic hydrolysis. The lipids were extracted by use of a low temperature enzymatic process without any organic solvent (Ackman, 1998). BF_3 (boron trifluoride)/methanol (purity = 99%) and hexane (purity = 97%) were used for gas chromatograph (GC) purchased from Sigma–Aldrich (France) and Fisher (France), respectively. These organic solvents were analytical grade reagents. Acetic acid (100%) and diiodomethane (99% GC) were supplied by prolabo – VWR and Aldrich (France), respectively.

2.2. Preparation of nanoliposomes

The procedure for preparing the nanoliposomes was as follows. First, three solutions of lecithin (extracted from soya, rapeseed and salmon head) were prepared by adding 2 g of lecithin into 38 mL of distilled water to obtain a 5% (w/w) lecithin solution for each. Then the solutions were continuously mixed for 4 h under inert atmosphere (nitrogen). Finally each solution was sonicated at 20 kHz and 200 W for 180 s (1 s on and 1 s off) to obtain colloidal suspensions. Nanoliposomes suspensions were stored in sterilized bottles in the dark at 4 °C and 1.013×10^5 Pa until preparation of nanoliposomes blend thin films.

2.3. Preparation of nanoliposome blend thin films

Chitosan was dissolved (2%, w/v) in 1% acetic acid solution, and stirred at room temperature. The solution was then filtered through a sintered glass filter (porosity: 100–160 μm) before being used. 10 mL of nanoliposomes solution were added in 90 mL of chitosan filtered solution and stirred at room temperature. Then 40 g of solution was casted into a 90 mm × 110 mm Petri dish and placed into an oven at 25 °C until dried. For a complete drying, the Petri dishes were then kept in a hermetic container containing P_2O_5 powder until used.

2.4. Cold plasma treatment

The plasma set-up is a home-made system whose details have been reported previously (Belmonte et al., 2005). The plasma reactor consists of a 5 mm inner diameter cylindrical quartz tube in which flows a $N_2/H_2/Ar$ gas mixture. The quartz tube crosses a 2.45 GHz microwave surfaguide (Moisan, Beaudry, & Lepprince, 1974) wave launcher (Fig. 1). Downstream the plasma, the post-discharge enters a Pyrex™ tube (28 mm inner diameter) 365 mm far away from the plasma gap. Such a long distance is necessary to prevent any effect of the pink afterglow in pure nitrogen.

Small size flat nanoliposomes functionalized chitosan samples (2 cm × 1 cm) were fixed on a metallic sample holder which was inserted in the post-discharge tube. This allowed us to precisely place the sample in the process chamber and avoided displacement of the light sample within the gas flow during the process.

The total flow rate was 1100 sccm (cm^3/min at 0 °C and 1.013×10^5 Pa; Ar: 1000 sccm, N_2: 50 sccm, H_2: 50 sccm). The total pressure was fixed at 400 Pa and the treatment time varied in the range of 50–300 s. The microwave power ranged from 150 to 450 W. The gas purities are 99.995%.

2.5. Experimental design

A Doehlert experimental design was adopted (Doehlert & Klee, 1972). The total number of points (N) for four factors (k) was 21 ($N \geq k^2 + k + 1$), and 25 experiments were carried out. The last five assays were performed at the center of the experimental domain in order to estimate the residual variance. The processing variables of plasma treatment investigated were microwave power (X_1, five levels), N_2/H_2 mixture gas ratio (X_2, seven levels), treatment time (X_3, seven levels), and distance between transmitting terminal and sample (X_4, three levels). The independent variables (X_i) and their levels are presented in Table 1.

2.6. Data analysis

For data analysis, ANalysis Of VAriance (ANOVA) and multiple linear regressions were performed using the NEMROD® software (Mazerolles, Mathieu, Phan-tan-luu, & Siouffi, 1989). A quadratic model containing 15 coefficients (Eq. (1)), including interaction terms, was assumed to describe relationships between the response Y and the experimental factors X_i:

$$Y = \beta_0 + \sum_{i=1}^{4} \beta_i X_i + \sum_{i=1}^{4} \beta_{ii} X_{ii}^2 + \sum_{i=1}^{3} \sum_{j=i+1}^{4} \beta_{ij} X_i X_j \quad (1)$$

where β_0 is the constant coefficient (intercept), β_i is the linear coefficient, β_{ii} is the quadratic coefficient, and β_{ij} is the second-order interaction coefficient.

Response surfaces and contour plots were developed using the fitted quadratic polynomial equations obtained from the response surface regression analysis. The level of significance for all tests was set at 95%. Numerous experimental and model prediction results of independent assays (Linder, Kochanowski, Fanni, & Parmentier, 2005; Riaño, Molinuevo, & García-González, 2012; Weska, Moura, Batista, Rizzi, & Pinto, 2007; Zhao et al., 2012) carried out to confirm

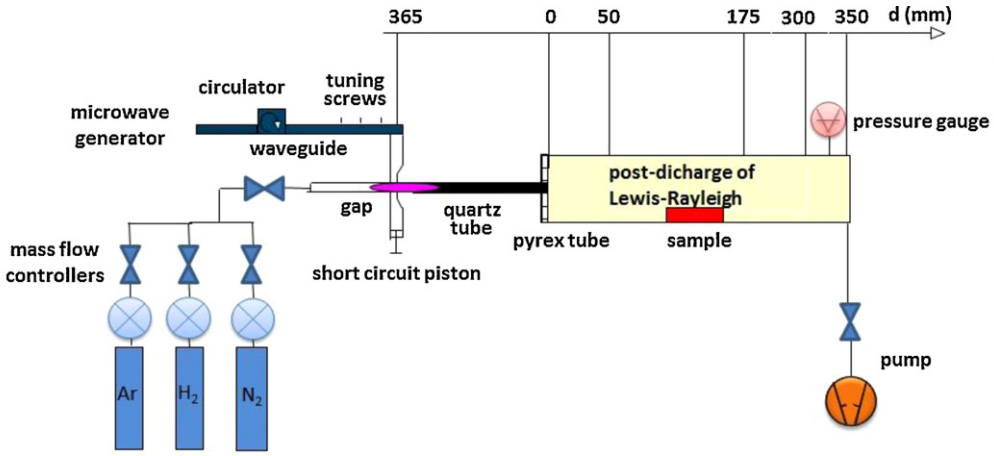

Fig. 1. Schema of Ar–H_2–N_2 microwave plasma plasma experimental setup. (For interpretation of the references to color in the text, the reader is referred to the web version of the article.)
Adapted from reference Belmonte et al. (2005).

the adequacy of the model predicted values at the optimal point were very close.

2.7. Characterization of nanoliposomes

2.7.1. Fatty acid composition

Fatty acid methyl esters (FAMEs) were prepared as described by Ackman (1998). The separation of the FAMEs was carried out using a Perichrom™ 2000 gas chromatograph (Perichrom, Saulx-lès-Chartreux, France), equipped with a flame-ionization detector. A fused silica capillary column was used (50 m, 0.25 mm inner diameter × 0.25 μm thin film thicknesses, CP 7419 Varian, Middelburg, Netherlands). Injector and detector temperatures were set at 260 °C. A column temperature was initially set at 145 °C for 5 min, then raised to 210 °C at a rate of 2 °C/min and held at 210 °C for 10 min. Standard mixtures (PUFA1 from marine source and PUFA2 from vegetable source; Supelco, Sigma–Aldrich, Bellefonte, PA, USA) were used to identify fatty acids. The results are presented as triplicate analyses.

2.7.2. Lipid class

The lipid classes of the different fractions were determined by Iatroscan MK-5 Thin Layer Chromatography coupled with Flame Ionization Detector (TLC-FID, Iatron Laboratories Inc., Tokyo, Japan). Each sample was spotted on ten Chromarod S-III silica coated quartz rods held in a frame. The rods were developed over 20 min in hexane/diethyl ether/formic acid (80:20:0.2, v/v/v), then oven dried for 1 min at 100 °C and finally scanned in the Iatroscan analyzer. The Iatroscan was operated under the following conditions: flow rate of hydrogen, 160 mL/min; flow rate of air, 2 L/min. A second migration using a polar eluent of chloroform, methanol, and ammoniac (65:35:5, v/v/v) made it possible to identify polar lipids. The FID results were expressed as the mean value of ten separate samples. The following standards were used to identify the sample components:

- Neutral lipids: 1-monostearoyl-rac-glycerol, 1,2-dipalmitoyl-snglycerol, tripalmitin, cholesterol.
- Phospholipids: L-α-phosphatidylcholine, 3-sn-phosphatidylethanolamine, L-α-phosphatidyl-L-serine, L-α-phosphatidylinositol, lyso-phosphatidylcholine, sphingomyelin.

All standards were purchased from Sigma (Sigma–Aldrich Chemie GmbH, Germany). The recording and integration of the peaks were provided by the ChromStar internal software.

2.7.3. Nanoliposomes size measurement

The various nanoliposomes sizes were analyzed by dynamic light scattering using a Malvern Zetasizer Nano ZS (Malvern instruments, UK). The apparatus was equipped with a 4 mW He/Ne laser emitting at 633 nm wavelength, measurement cell, photomultiplier and correlator. The samples were diluted in ultra-filtrate distilled water (1:400) and placed in vertical cylindrical cells (10 mm diameters). The scattering intensity was measured at a scattering angle of 173° relative to the source, using a photodiode detector, at 25 °C. Intensity autocorrelation functions were analyzed by a General Purpose Algorithm (integrated in the Malvern Zetasizer software) in order to determine the distribution of the translational z-averaged diffusion coefficient of the particles, D_T ($m^2\ s^{-1}$). The D_T parameter is related to the hydrodynamic radius (R_h) of particles through the Stokes–Einstein relationship $D_T = k_B T/(6\pi\eta R_h)$. During dispersion, particles are in a constant Brownian motion, so it causes the intensity of scattered light to fluctuate as a function of time. Therefore, droplets sizes were obtained from the correlation function calculated by the Dispersion Technology Software (DTS) using various algorithms. The Refractive Index (RI) and absorbance were fixed

Table 1
Experimental domain and level distribution variables used for minimization the water contact angle.

Independent variables	Symbol	Experimental values	Levels
Microwave power (W)	X_1	150, 225, 300, 375, 450	5
N_2/H_2 mixture gas ratio (N_2%)[a]	X_2	0, 17, 33, 50, 67, 83, 100	7
Treatment time (s)	X_3	50, 81, 144, 175, 206, 269, 300	7
Distance between transmitting terminal and sample (mm)	X_4	50, 175, 300	3

[a] The flow rate of Ar is always 1000 sccm.

respectively at 1.471 and 0.01 at 25 °C. The measurements were carried out in five repetitions.

2.7.4. Electrophoretic mobility

Electrophoretic mobility measurements (μE) were performed by means of laser Doppler electrophoresis. The sample was placed in a standard capillary electrophoresis cell equipped with gold electrodes. The electrophoretic mobility of nanoliposomes was realized out to evaluate the surface net charge around lipid droplets. To avoid multiple scattering effects, the nanoliposomes were diluted with deionized water prior to analysis and then directly placed into the module. Measurements were performed directly in the diluted nanoliposomes suspensions and results were presented as triplicate analyses.

2.8. Thin films characterization methods before and after plasma treatment

2.8.1. Mass variation

Weight gain of sample due to the plasma treatment was determined from mass measurements (with an accuracy of 0.1 mg) before and after plasma processing. Once the film was treated, it was preserved in an ice bag and in the dark before characterization by different techniques described hereafter. The mass variation ratios are defined by the difference $(m - m_0)/m_0$ expressed in mg where m_0 was the initial mass of the sample before treatment and m was the mass after treatment.

2.8.2. Contact angle measurement

Contact angle measurements of chitosan and nanoliposomes blend thin films were performed by following the sessile drop method with a contact angle instrument (Digidrop Contact AngleMeter) equipped with an image analysis attachment (Windrop). The probe liquids used were milli-Q® water. Uniform drops of liquids (0.75 μL) were carefully deposited on the blend film verso side (contact surface with Petri™ dish) using micrometer syringe. The volume of the drops was kept constant since variations in the volume of the drops can lead to inconsistent contact angle measurements. Measurements were consistently conducted under the constant conditions of relative humidity (39%) and temperature (23 °C). Contact angle measurements were recorded three times on three different locations on the verso side within 5 s for a given blend thin film.

2.8.3. Surface energy measurement

The total surface energy of the films was determined graphically by the Owens–Wendt method, which is usually applied for solids with low surface energy such as polymers. The Owens–Wendt theory divides the surface energy into two components: surface energy due to dispersive interactions and surface energy due to polar interactions (Rotta et al., 2009). Owens and Wendt proved that the total surface energy of a solid, γ_S^T can be expressed as the sum of contributions from dispersion γ_S^d and polar γ_S^p force components. The Owens–Wendt equation (Eqs. (2) and (3)) applies the contact angle, θ, data of polar and non-polar liquids with known dispersion γ_L^d and polar γ_L^p parts of their surface energy, via the following relations:

$$\gamma^T = \gamma^d + \gamma^p \quad (2)$$

$$\gamma_L(1 + \cos\theta) = 2\sqrt{\gamma_S^d}\sqrt{\gamma_L^d} + \sqrt{\gamma_S^P}\sqrt{\gamma_L^P} \quad (3)$$

where γ_L is the liquid surface tension.

For this measurement, four liquids including water, glycerol, ethylene glycol and diiodomethane tested for each film at 23 °C and 50% RH.

The same Digidrop meter apparatus was used for measuring surface energies of chitosan and blend films. The total surface energy, polar component and dispersion component of chitosan and nanoliposomes blend thin films have been determined before and after plasma treatment from the water and diiodomethane contact angle; only the water contact angle is reported in Table 2a.

2.8.4. X-ray photoelectron spectroscopy

The X-ray photoelectron spectroscopy (XPS) analyses were carried out with a Kratos Axis Ultra spectrometer using a monochromatic Al Kα source. All spectra were recorded at 90° take-off angle. Analyzed area was about 700 μm × 300 μm. Survey spectra were recorded with 1.0 eV step and 160 eV analyzer pass energy. High resolution regions were scanned with 0.1 eV step and 20 eV pass energy except for carbon (0.05 eV step). In both cases, the hybrid lens mode was employed (magnetic and electrostatic). During data acquisition the Kratos charge neutralizer system was used on all specimens with the following settings: filament current 2 A, charge balances 3.5 V, filament bias 1.0 V and magnetic lens trim coil 0.34 A. The C—(C, H) carbon was set to 284.60 eV and therefore used as an internal energy reference. Spectra were analyzed using the Vision software from Kratos (Vision 2.2.6). A Shirley base line was used for the subtraction of the background from each peak. Quantification was performed using the photoemission cross sections and transmission coefficients given in the vision package.

2.8.5. Intermittent contact-atomic force microscopy (IC-AFM)

Chitosan and nanoliposomes blend thin film surface morphology were analyzed in air under ambient conditions at 37 °C using a Dimension 3100 with a NanoScopeV controller. The images were recorded in soft intermittent contact atomic force microscopy analysis (also called Tapping™ mode). Tap 150 tapping mode cantilevers (Veeco model No. Mpp-12100-10), with a typical spring constant of 5 N/m and a resonance frequency at 137 kHz, were used for scanning. The image quality depends on the scan rate which was adjusted in the range of 0.4–0.8 Hz. For acquisition of the surface morphology, height and amplitude error images were recorded on 3 areas of each film. Only the height images were discussed with a scan size of 5 μm^2.

All offline image flattening and analyses were conducted with the software environment provided by the AFM manufacturer. The statistical parameters related with sample roughness (ASME B46.1. 2002) were estimated by the equipment software including: average roughness (R_a), root mean square roughness (R_q), skewness (S_k) and kurtosis (E_k).

3. Results and discussion

3.1. Characterization of nanoliposomes

3.1.1. Fatty acid analysis

The main fatty acid composition analysis showed that the percentage of total PUFAs was the highest in soya lecithin, but the salmon lecithin has the most variety of PUFAs. Indeed, we observed nine PUFAs of omega 3 and omega 6 in this lecithin.

The most significant proportions of fatty acids were C18:2 (n-6), found in the PUFAs class, C18:1 (n-9) in the monounsaturated fatty acids class and C16:0 in the saturated fatty acids class for soya lecithin. The most important fatty acid was C18:1 (n-9) with 55.78% for rapeseed lecithin in the monounsaturated fatty acid. For salmon lecithin, the results showed that the main percentage of unsaturated fatty acids are C22:6 (n-3) and C20:5 (n-3) with 10.78% and 6.71%, respectively.

Table 2
Comparison of (a) contact angle, mass variation and (b) surface energy of chitosan and blend films before and after plasma treatment.

(a) Contact angle, mass variation

	N_2/H_2	Average of water contact angle (°)		Mass variation (mg)
		Before	After	$(m-m_0)/m_0$
Pure chitosan	0/100	**101 ± 2**	95 ± 5	0.07% ± 0.02%
	50/50		76 ± 4	1.07% ± 0.13%
	88/12		**27 ± 5**	**0.66% ± 0.17%**
	100/0		34 ± 1	2.25% ± 0.09%
ns-chitosan	0/100	**82 ± 2**	81 ± 12	0.91% ± 0.07%
	50/50		57 ± 3	0.38% ± 0.04%
	88/12		62 ± 2	0.88% ± 0.21%
	100/0		**57 ± 4**	**2.57% ± 0.03%**
nr-chitosan	0/100	**69 ± 2**	67 ± 5	0.98% ± 0.06%
	50/50		65 ± 7	0.68% ± 0.12%
	88/12		**57 ± 5**	**0.81% ± 0.16%**
	100/0		68 ± 12	0.32% ± 0.14%
nf-chitosan	0/100	**64 ± 2**	94 ± 3	0.96% ± 0.16%
	50/50		65 ± 10	0.71% ± 0.22%
	88/12		68 ± 2	1.1% ± 0.17%
	100/0		**34 ± 1**	**0.82% ± 0.34%**

(b) Surface energy of chitosan and blend films before and after plasma treatment

Owens–Wendt equation	Before plasma treatment			N_2/H_2	After plasma treatment		
	Total energy γ^T (mJ/m²)	Polar component γ^p (mJ/m²)	Dispersive component γ^d (mJ/m²)		Total energy γ^T (mJ/m²)	Polar component γ^p (mJ/m²)	Dispersive component γ^d (mJ/m²)
Pure chitosan	**30.5 ± 0.4**	0.9 ± 0.4	29.6 ± 0.8	0/100	37.2 ± 2.1	3.6 ± 2.8	33.5 ± 0.9
				50/50	60.1 ± 6.0	21.5 ± 5.4	38.6 ± 0.5
				88/12	**175.3 ± 8.8**	144.7 ± 8.9	30.6 ± 0.2
				100/0	152.7 ± 1.3	116.3 ± 1.9	36.4 ± 0.6
ns-chitosan	**46.4 ± 0.4**	16.0 ± 0.4	30.4 ± 0.0	0/100	66.4 ± 5.9	35.9 ± 6.5	30.4 ± 1.0
				50/50	107.3 ± 13	76.0 ± 12.5	31.3 ± 1.1
				88/12	92.6 ± 5.5	62.9 ± 6.8	29.7 ± 1.3
				100/0	**104.7 ± 9.6**	74.3 ± 8.8	30.3 ± 0.8
nr-chitosan	**81.1 ± 4.3**	58.2 ± 4.3	22.8 ± 0.0	0/100	77.6 ± 11.4	43.2 ± 11.0	34.3 ± 1.5
				50/50	82.0 ± 15.5	49.2 ± 13.8	32.8 ± 1.9
				88/12	**99.3 ± 12.6**	64.2 ± 13.4	35.1 ± 1.0
				100/0	82.7 ± 18.7	49.5 ± 18.8	33.2 ± 1.8
nf-chitosan	**81.8 ± 2.4**	50.6 ± 2.0	31.2 ± 0.4	0/100	36.9 ± 2.1	4.8 ± 2.1	32.1 ± 0.5
				50/50	84.2 ± 24.0	54.2 ± 23.4	30.0 ± 0.7
				88/12	75.5 ± 3.5	41.9 ± 3.7	33.6 ± 0.2
				100/0	**163.1 ± 1.5**	133.2 ± 2.3	29.9 ± 1.1

ns, nr, nf-chitosan: soya, rapeseed, fish nanoliposomes blend thin film. Bold values highlighted significant differences of mass and wettability before and after plasma treatment only when the N_2/H_2 mixture gas ratio was set to 88/12%, and 100/0%.

3.1.2. Lipid classes

The lipid classes of lecithins were separated by thin-layer chromatography (Iatroscan). At that stage, salmon lecithin contains 38.9 ± 0.8% of triacylglycerols (TAG) and 61.1 ± 0.2% of polar fraction. Phosphatidylcholine (PC) thus represented the major class of phospholipids contained in salmon lecithin (33%). The percentage of polar fraction and TAG for rapeseed lecithin were 71.3 ± 0.5% and 28.7 ± 0.1% respectively. The soya lecithin was found to be richer in polar lipids (81.9 ± 0.3%) than other lecithins and that its TAG percentage was 18.2 ± 0.2%.

3.1.3. Nanoliposomes size measurement

The particle sizes of the different nanoliposomes were measured immediately after sonication by Zetasizer. The minimum achievable size generally depends on material viscosity and on applied sonication parameters (amplitude and time). In our study, the sizes of the nanoliposomes are presented in diameter. The average diameter of the nanoliposomes was 129 ± 2 nm and polydispersity index was 0.46 for particles from fish lecithin. The average diameters of the nanoliposomes for rapeseed and soya lecithin were 174 ± 10 nm and 190 ± 3 nm, respectively. Compared to fish lecithin, the polydispersity index was lower for rapeseed lecithin, with an index of 0.28, and for soya lecithin, with an index of 0.25. The results show, the percentage of mono and poly-unsaturated fatty acids varied according to the lecithin source. We observed that soja lecithin contains a high percentage of PUFAs with 57.3% in comparison to rapeseed and fish lecithin with 31.5% and 36.2%, respectively. An increased ratio of PUFAs consequently increased the size of the nanoliposomes. In addition, the ratio of Long Chain PUFAs (LC-PUFAs) such as EPA and DHA changed the size of nanoliposomes. By increasing the LC-PUFAs ratio in lecithin, the size of nanoliposomes increased and the polydispersity index increased. Thus, it was clear that the size of the nanoliposomes depended not only on such physical parameters as the amplitude of sonicator (Alvarez, Seyler, Madrigal-Carballo, Vila, & Molina, 2007), but also on the composition of lecithin.

3.1.4. Electrophoretic mobility

Measurements of electrophoretic mobility vary between −3 and −5 μm cm/V s with a relatively high stability of the formulations.

Table 3
Regression coefficients of predicted second-order polynomial model for variables responses.

Variables		Coefficients (β) for water contact angle
Intercept		33.753[b]
Linear	X_1	−5.317[b]
	X_2	−20.404[b]
	X_3	−19.772[b]
	X_4	2.662[a]
Quadratic	X_{11}	51.590[b]
	X_{22}	17.803[b]
	X_{33}	25.668[b]
	X_{44}	4.259
Interaction	X_{12}	−3.816
	X_{13}	−15.996[b]
	X_{23}	−0.931
	X_{14}	−5.247
	X_{24}	−13.999[b]
	X_{34}	−6.724

[a] $1\% < \alpha < 5\%$.
[b] $\alpha \leq 1\%$.

This is mainly due to the positive and negative charge brought by the polar fraction of lecithin (Section 3.1.2). According to the results obtained from Zetasizer, the electrophoretic mobility is higher in soya lecithin (−5 μm cm/V s) than for rapeseed (−3.6 μm cm/V s) and fish (−3.1 μm cm/V s) lecithin. One can notice that the value of electrophoretic mobility is negative throughout the storage period regardless of the type of formulation. The salmon, soya and rapeseed lecithin contain different types of phospholipids such as phosphatidylserine (PS), phosphatidic acid (PA), phosphatidylglycerol (PG), phosphatidylinositol (PI), phosphatidylethanolamine (PE), and PC. At physiological pH these phospholipids are negatively charged, except the PC which exhibits no global charge. Thus, these anionic fractions are probably responsible for the negative electrophoretic mobility (Chansiri, Lyons, Patel, & Hem, 1999). PC represented the major class of phospholipids contained in salmon lecithin (33%), rapeseed lecithin (30%) and soya lecithin (14%).

3.2. Plasma treatment

Compared to the untreated films, the wettability of pure chitosan films after N_2/H_2 mixture gas treatment was enhanced. The surface energy of the N_2/H_2 mixture gas modified films was evaluated by water contact angle measurements. Table 3 shows the respective regression coefficients of predicted second-order polynomial model for pure chitosan film which was treated by plasma. From the obtained results, we observed that X_2 (N_2/H_2 mixture gas ratio) and X_3 (treatment time) were the most influential negative parameters. It means that water contact angle is highly sensitive to these two parameters. We can observe that a minimum water contact angle (around 20°) was obtained under the following conditions: microwave power 334 W, N_2/H_2 mixture gas ratio 88% N_2 and 12% H_2, treatment time 251 s, distance between transmitting terminal and sample 260 mm (Fig. 2). Further to these results on pure chitosan films, blend thin films were plasma processed with four different N_2/H_2 gas mixture ratios which were respectively: 0/100%, 50/50%, 88/12% and 100/0%. All other plasma parameters were set at their optimal value as determined in the case of pure chitosan film.

3.3. Thin films characterization before and after plasma treatment

3.3.1. Mass variation

Compared to the pure chitosan thin films, we observed an increased mass variation (Table 2a) for the nanoliposomes blend thin films after the treatment. Specially, we noticed that the soya nanoliposomes make the pure chitosan thin films gain more mass than the other nanoliposomes. That is because the large quantities of PUFAs presented in soya nanoliposomes which increase the mobility of pure chitosan films.

3.3.2. Contact angle measurements

The surface wettability of films was measured by contact angle analysis using water. The films with smaller contact angle value have the better surface wettability. We can observe in Table 2a that before plasma treatment, the water contact angle of nanoliposomes

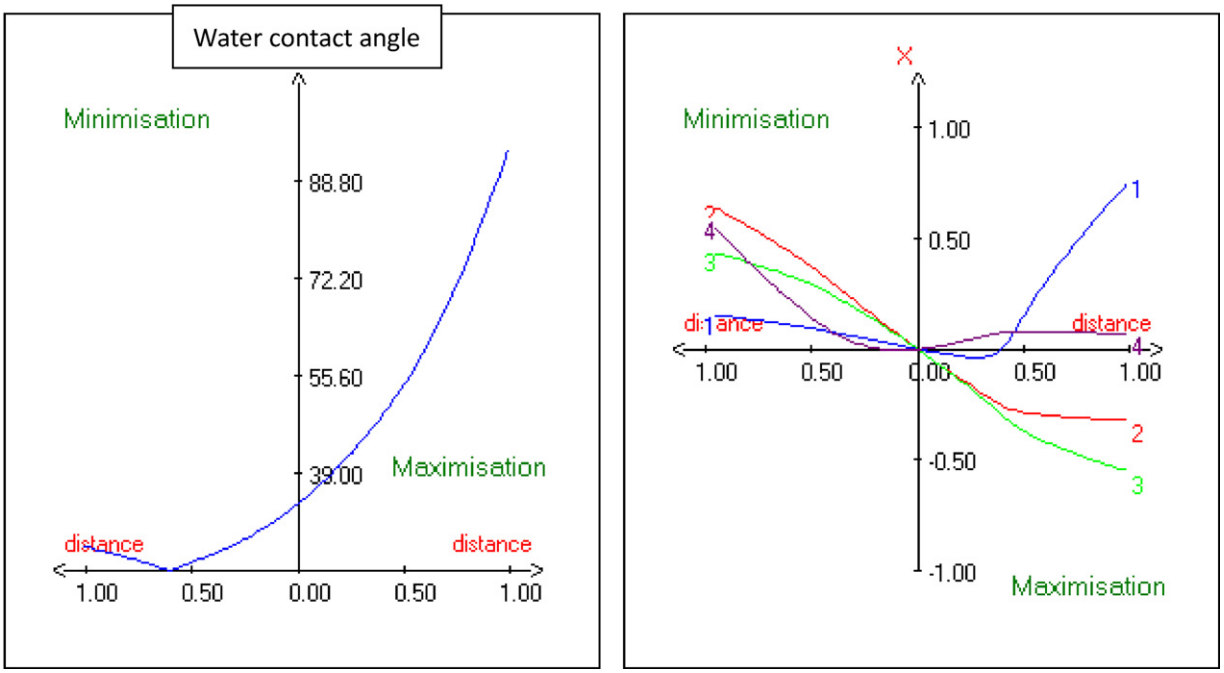

Fig. 2. Optimization of water contact angle using a Doehlert experimental design: optimal pathway to optimize the different factors simultaneously, to decrease the water contact angle (microwave power (X_1); N_2/H_2 mixture gas ratio (X_2); treatment time (X_3); distance between transmitting terminal and sample (X_4)).

Table 4
XPS analysis of surface elemental composition and possible groups of non-treated chitosan and plasma treated chitosan films with different gas mixture.

	Samples	O	N	C	O=C	O—C O—H	C—(C, H)	C—O	C=O	O—C=O	C—(NH, NH_2)	C—NH_3
Before plasma	Pure chitosan	7.10	1.45	91.44	12.37	87.63	70.01	10.34	–	1.74	–	–
	ns-chitosan	13.76	0.64	85.05	10.97	62.30	62.37	17.23	–	3.39	–	–
	nr-chitosan	10.50	0.63	88.15	11.27	56.50	49.14	13.80	–	2.84	–	–
	nf-chitosan	21.58	4.66	72.49	6.68	93.32	51.83	34.36	9.49	4.32	82.96	17.04
After plasma	Pure chitosan 0%N_2/100%H_2	32.71	7.81	59.47	16.61	77.48	17.93	58.15	19.43	4.49	75.30	24.70
	Pure chitosan 50%N_2/50%H_2	28.04	6.45	65.38	22.93	71.26	34.54	44.82	16.58	4.05	68.38	31.62
	Pure chitosan 88%N_2/12%H_2	33.47	8.60	57.56	16.68	76.57	16.47	56.79	21.30	5.43	76.46	23.54
	Pure chitosan 100%N_2/0%H_2	31.73	10.74	57.53	19.40	77.00	20.23	53.68	21.18	4.91	81.23	18.77
	ns-chitosan 100%N_2/0%H_2	18.29	4.80	76.06	21.57	56.63	69.60	14.43	7.52	8.45	–	–
	nr-chitosan 88%N_2/12%H_2	14.72	5.18	79.86	16.26	55.73	72.47	13.58	6.41	7.55	–	–
	nf-chitosan 100%N_2/0%H_2	25.67	7.40	65.04	18.27	75.45	43.71	35.86	13.51	6.92	–	–

ns, nr, nf-chitosan: soya, rapeseed, fish nanoliposomes blend thin film.

blend thin films is smaller than that of the pure chitosan film whatever the origin of nanoliposomes. Among all films, the films based on rapeseed and fish lecithin presented a much smaller contact angle than the others. Among these results, we found that the fish lecithin is the more efficient lecithin to decrease the film contact angle. That is probably due to the amount of the variety of the PUFAs (Section 3.1.1) and its polar lipid proportion (Section 3.1.2).

Moreover, for the pure chitosan and the rapeseed nanoliposomes blend thin films, it exists significant statistical differences for water contact angle before and after plasma treatment only when the N_2/H_2 mixture gas ratio was set to 88/12%, and 100/0%. Thus, for pure chitosan, soya and fish nanoliposomes blend films, the wettability of the films increases with increasing the N_2 ratio in the gas mixture (Section 3.2), but for rapeseed nanoliposomes blend films, the wettability is stable even increasing the N_2 ratio in the gas mixture.

3.3.3. Surface energy measurement

Regarding the total surface energy before plasma treatment (Table 2b), we can notice that this property changed significantly. The total surface energy and polar component of nanoliposomes blend thin films have significantly increased compared to the pure chitosan thin film. After plasma treatment with N_2/H_2 mixture gas ratio set to 88/12%, we can observe that total surface energy of pure chitosan thin films widely increased (six times) in compared to films before the treatment. When the N_2/H_2 mixture gas ratio was set to 100/0%, total surface energy of soya and fish nanoliposome blend thin films doubled compared to the untreated film. And total surface energy of rapeseed nanoliposomes blend thin films slightly raised when the N_2/H_2 mixture gas was ratio equal to 88/12%. It means, although being a temporary affect (König et al., 2002; Morra et al., 1989; Vesel & Mozetic, 2012), the plasma could be used as an efficient treatment method for increasing the surface energy.

From these results, we could conclude that plasma treatment graft polar composition (amine groups) on the surface, the wettability improved due to an increasing of polar component. Further, we could always compare these results with what we got in Section 3.2.

3.3.4. X-ray photoelectron spectroscopy

X-ray photoelectron spectroscopy (XPS) analysis was performed to examine the energy changes and chemical binding states of the polymer surfaces. Usually the surface modification is an intermediate case, only the outermost layers (some 10 nm) of a surface are modified by plasma treatment due to numerous parameters (König et al., 2002). Therefore, extremely sensitive surface techniques have to be applied to obtain information on surface modifications at a molecular level. In this investigation, the chemical composition of the sample surface was determined using XPS (Gray, Norton, & Griffiths, 2003; König et al., 1999).

According to Table 4, the atomic composition of chitosan films after adding the nanoliposomes based on soya, rapeseed, and fish change before plasma treatment. An increase in the O 1s peak can be seen, which indicates the incorporation of oxygen onto the sample surface after incorporation of lecithin. This increase is much pronounced for fish nanoliposomes.

The C, O, and N peaks were decomposed according to a model for biochemical compounds (Fig. 3). The C 1s peak was decomposed in three distinct peaks: a peak at 284.60 eV corresponding to C—(C, H) bond, a peak at 286.61 eV due to C—O and O—C=O functions. The O 1s peak was decomposed in two peaks attributed to the O=C at 531.27 eV and O—C, O—H at 532.74 eV. The N 1s peak was decomposed in C—(NH, NH_2) and C—NH_3 at 401.62 eV.

The pure chitosan thin film has a high concentration of C 1s. We observed a significant decrease in C 1s for fish nanoliposomes blend thin films. The fish nanoliposomes increase significantly these polar functional groups. By decreasing the C/O ratio, the hydrophobicity of the chitosan thin films decreases. Thus, the nanoliposomes incorporation increases the wettability of surface. The results of contact angle measurements confirmed the XPS results. Table 4 clearly shows that the concentration of the C—(C, H), C—O and O—C=O bonds increased after nanoliposomes incorporation.

In addition, XPS analysis was performed to examine the energy changes and chemical binding states of the polymer surfaces after plasma treatment. Table 4 shows the surface modification of N_2/H_2 plasma treated pure chitosan thin films. Compared with untreated pure chitosan thin films, the O 1s and N 1s concentrations increased significantly while C 1s was strongly lowered. After the plasma treatment, the intensities of the three peaks related to the C—O, C=O, and O—C=O increased, while the O—C O—H, and C—(C, H) peaks' intensities decreased. This indicates that the pure chitosan thin films were broken by reactive species in the plasma post-discharge, and the decomposed bonds subsequently preferred to create an unsaturated and unstable C=O functional groups upon the surface.

According to Table 4, we observed also that the higher rate of N_2 in the gas mixture increased the surface erosion and the etching is accentuated. The following results are confirmed by mass variation (see Table 2a). By increasing the percentage of N_2, the radicals created by the plasma are very unstable, they re-associate themselves, and so, it remains only a few free radicals which are able to obtain the created radicals in post-discharge. This would explain the increase in the energy of polar compounds and effect of aging observed.

Comparing to untreated nanoliposomes blend thin films, the treated thin films had more important O 1s and N 1s concentrations. The plasma treatment caused the increase in the functional groups such as C=O and C—O except for the fish nanoliposomes blend thin films.

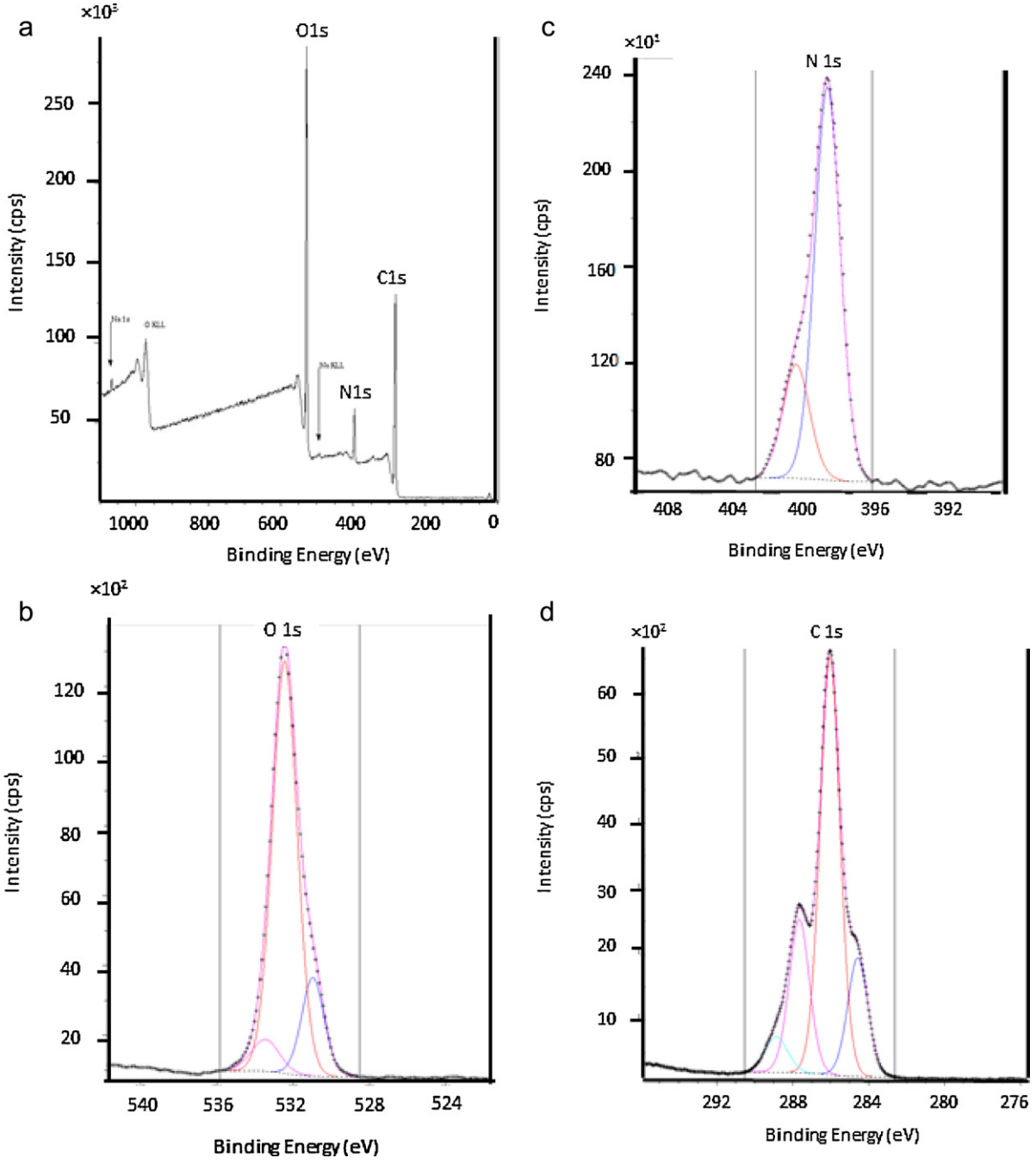

Fig. 3. Example of XPS spectra obtained for chitosan films: (a) survey scan; (b–d) narrow spectra of O 1s, N 1s and C 1s levels, respectively.

Thanks to XPS analysis, we observed that the lecithin and gas composition were the two most influent parameters. The effect of lecithin on surface composition depends on lecithin composition. The results showed that fish lecithin improved the contact angle and surface energy of the pure chitosan thin films. According to XPS results, we can confirm the grafting of the functional groups upon the chitosan thin film surface. Whereas, the modification in surface composition is less important compared to soya and rapeseed lecithin. These differences could be explained by the fatty acids composite type of each lecithin. Soya and rapeseed lecithin have the same type of fatty acids in different proportion (soya lecithin is composed most of unsaturated fatty acids). However, the fish lecithin has a great influence on the surface composition because it is rich in PUFAs.

3.3.5. Intermittent contact-atomic force microscopy (IC-AFM)

As Vesel and Mozetic (2012) observed, besides chemical changes on the surface, plasma treatment also induced some morphological modifications of the surface. Fig. 4a, c, e and g represents height images of pure chitosan and nanoliposomes blend thin films before plasma treatment. Pure chitosan films (Fig. 4a) reveals some higher structural entities in the topography signal in comparison with the other blend films and has a rougher surface with R_a = 15.9 nm, R_q = 20.2 nm. In addition, we have not observed different microstructures in the phase images. It means that the phase signal give a better lateral contrast unveiling more details of the morphology than the height signals. As a result, the chitosan thin films roughness was decreased through the filling of nanoliposomes. This effect has been proved by the roughness values in Fig. 4.

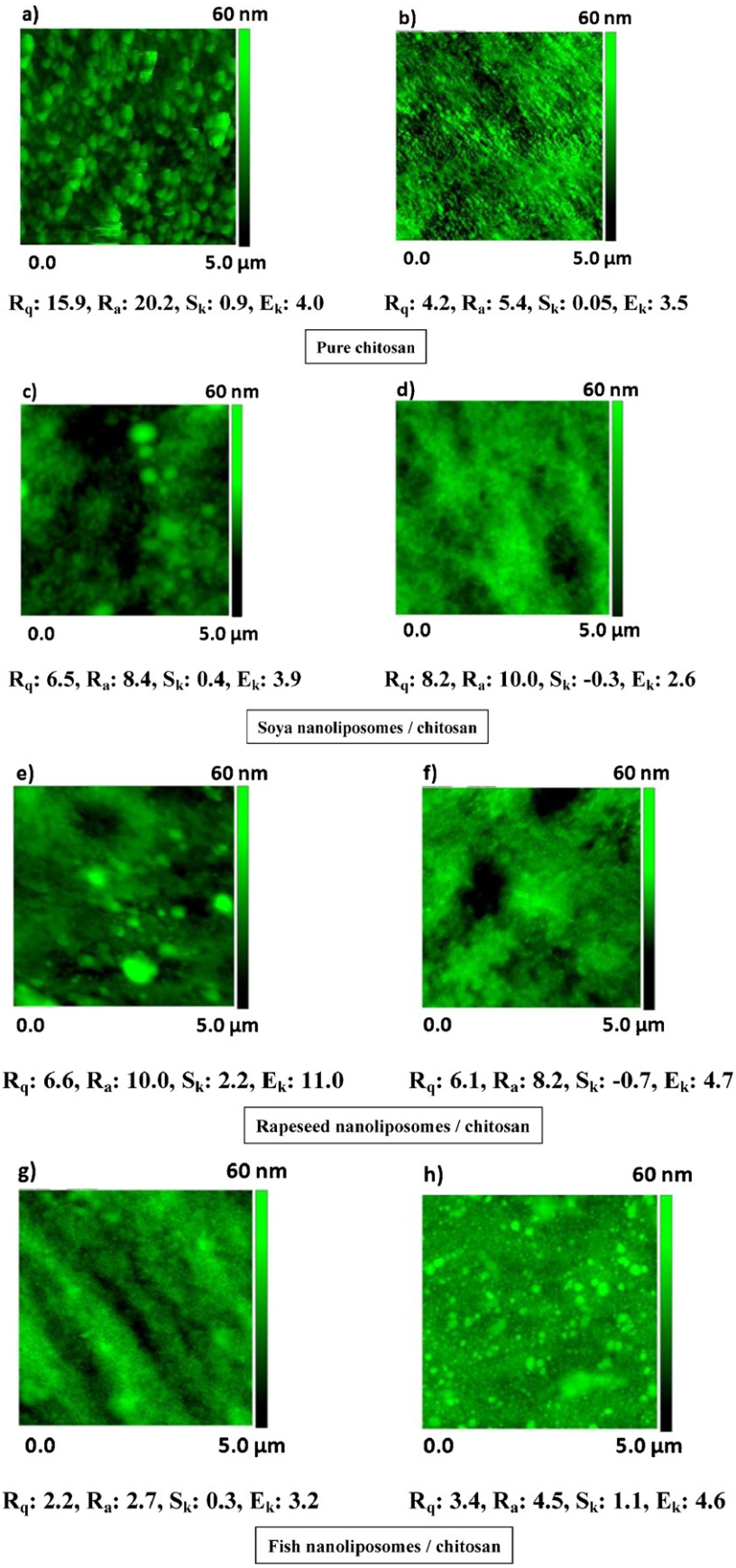

Fig. 4. SPM Tapping™ mode height images and surface roughness (nm) of pure chitosan, soya, rapeseed, and fish nanoliposomes/chitosan thin film surfaces before plasma treatment ((a), (c), (e), and (g)); and after plasma treatment ((b), (d), (f), and (h)).

This variation in roughness should also be correlated to XPS measurements (Table 4). Indeed, the higher the O 1s and N 1s grafted upon the film, the less roughness of the nanoliposomes blend thin films can be founded.

Fig. 4b, d, f, and h shows that the surface microstructure of films was affected differently by plasma treatment. Indeed, the roughness of pure chitosan film is lowered by a factor greater than 4 by the plasma processing with R_a = 4.2 nm and R_q = 5.4 nm. But, there is no evident roughness variation for nanoliposomes blend thin films compared to that before plasma treatment. Thus, it is necessary to compare the variation of complementary parameters, especially the profile symmetry/height balance, via both S_k and E_k parameters. The plasma treatment decreases evidently S_k value of soya and rapeseed nanoliposomes thin films, but not the fish nanoliposomes thin films. Moreover, we do not observe any significant E_k variation for soya and fish nanoliposomes thin films, but there is a very important E_k variation for rapeseed nanoliposomes thin films. We could conclude that these variations are due to the different component of lecithins, the details need to be proved by future experiments.

4. Conclusions

This paper describes the effects of different plasma treatments ($Ar/N_2/H_2$) on chitosan and nanoliposomes blend thin films focusing on the chemical and physical modifications induced on the surface.

Using a plasma gas mixture, functional groups are grafted onto the surface and enhance the surface energy of the films. The effect of plasma treatment depends on the nature of the film, especially on the type of nanoliposomes that is used to functionalize the chitosan films. It also supplied more efficiency and more advantages than nanoliposomes incorporation for increasing the surface wettability. However, the stability of the plasma treatment effect depends on the environmental conditions during storage time. Hydrogen bonds between the polar groups introduced by the treatment can be vanished after a given time, which can explain why many researchers failed to find improved wettability in their treated samples. This drawback may limit the application of this proceeding in tissue engineering. Or, it must be used in complement with another functionalization treatment for reducing the water contact angle such as the incorporation of nanoliposomes from lecithins in the biopolymers.

Acknowledgement

We would like to thank Mrs. Marie-Cécile De weerd for her advice and assistance in contact angle and surface energy measurement.

References

Ackman, R. (1998). Remarks on official methods employing boron trifluoride in the preparation of methyl esters of the fatty acids of fish oils. *Journal of the American Oil Chemists' Society*, *75*(4), 541–545.

Alvarez, M. A., Seyler, D., Madrigal-Carballo, S., Vila, A. O., & Molina, F. (2007). Influence of the electrical interface properties on the rheological behavior of sonicated soy lecithin dispersions. *Journal of Colloid and Interface Science*, *309*(2), 279–282.

ASME B46.1-2002. Surface Texture (Surface Roughness, Waviness and Lay), American Society of Mechanical Engineers, 1995.

Belhaj, N., Arab-Tehrany, E., & Linder, M. (2010). Oxidative kinetics of salmon oil in bulk and in nanoemulsion stabilized by marine lecithin. *Process Biochemistry*, *45*(2), 187–195.

Belmonte, T., Pintassilgo, C. D., Czerwiec, T., Henrion, G., Hody, V., Thiebaut, J. M., et al. (2005). Oxygen plasma surface interaction in treatments of polyolefines. *Surface and Coatings Technology*, *200*(1–4), 26–30.

Bhardwaj, N., & Kundu, S. C. (2011). Silk fibroin protein and chitosan polyelectrolyte complex porous scaffolds for tissue engineering applications. *Carbohydrate Polymers*, *85*(2), 325–333.

Casettari, L., Vllasaliu, D., Castagnino, E., Stolnik, S., Howdle, S., & Illum, L. (2012). PEGylated chitosan derivatives: Synthesis, characterizations and pharmaceutical applications. *Progress in Polymer Science*, *37*(5), 659–685.

Chansiri, G., Lyons, R. T., Patel, M. V., & Hem, S. L. (1999). Effect of surface charge on the stability of oil/water emulsions during steam sterilization. *Journal of Pharmaceutical Sciences*, *88*(4), 454–458.

Chen, C., Liang, B., Lu, D., Ogino, A., Wang, X., & Nagatsu, M. (2010). Amino group introduction onto multiwall carbon nanotubes by NH_3/Ar plasma treatment. *Carbon*, *48*(4), 939–948.

Coonrod, D., Brick, M., Byrne, P., DeBonte, L., & Chen, Z. (2008). Inheritance of long chain fatty acid content in rapeseed. *Euphytica*, *164*(2), 583–592.

Dash, M., Chiellini, F., Ottenbrite, R. M., & Chiellini, E. (2011). Chitosan—A versatile semi-synthetic polymer in biomedical applications. *Progress in Polymer Science*, *36*(8), 981–1014.

Doehlert, D. H., & Klee, V. L. (1972). Experimental designs through level reduction of the d-dimensional cuboctahedron. *Discrete Mathematics*, *2*(4), 309–334.

Domard, A. (2011). A perspective on 30 years research on chitin and chitosan. *Carbohydrate Polymers*, *84*(2), 696–703.

Duarte, A. R. C., Mano, J. F., & Reis, R. L. (2010). Novel 3D scaffolds of chitosan–PLLA blends for tissue engineering applications: Preparation and characterization. *The Journal of Supercritical Fluids*, *54*(3), 282–289.

Gray, J. E., Norton, P. R., & Griffiths, K. (2003). Surface modification of a biomedical poly(ether)urethane by a remote air plasma. *Applied Surface Science*, *217*(1–4), 210–222.

Hody, V., Belmonte, T., Czerwiec, T., Henrion, G., & Thiebaut, J. M. (2006). Oxygen grafting and etching of hexatriacontane in late N_2–O_2 post-discharges. *Thin Solid Films*, *506*, 212–216.

Hody, V., Belmonte, T., Pintassilgo, C., Poncin-Epaillard, F., Czerwiec, T., Henrion, G., et al. (2006). Modification of hexatriacontane by O_2–N_2 microwave post-discharges. *Plasma Chemistry and Plasma Processing*, *26*(3), 251–266.

Hoemann, C. D., Sun, J., Légaré, A., McKee, M. D., & Buschmann, M. D. (2005). Tissue engineering of cartilage using an injectable and adhesive chitosan-based cell-delivery vehicle. *Osteoarthritis and Cartilage*, *13*(4), 318–329.

Inagaki, N., Narushima, K., Hashimoto, H., & Tamura, K. (2007). Implantation of amino functionality into amorphous carbon sheet surfaces by NH_3 plasma. *Carbon*, *45*(4), 797–804.

Ji, C., Annabi, N., Khademhosseini, A., & Dehghani, F. (2011). Fabrication of porous chitosan scaffolds for soft tissue engineering using dense gas CO_2. *Acta Biomaterialia*, *7*(4), 1653–1664.

König, U., Nitschke, M., Menning, A., Sperling, C., Simon, F., Arnhold, C., et al. (1999). Plasma modification of polytetrafluoroethylene for immobilization of the fibrinolytic protein urokinase. *Surface and Coatings TechnologyV 116–119*, 1011–1015.

König, U., Nitschke, M., Pilz, M., Simon, F., Arnhold, C., & Werner, C. (2002). Stability and ageing of plasma treated poly(tetrafluoroethylene) surfaces. *Colloids and Surfaces B: Biointerfaces*, *25*(4), 313–324.

Kral, M., Ogino, A., & Nagatsu, M. (2008). Effect of Ar and N_2 plasma pretreatment with biased sample holder on amino group introduction on to polyethylene sheet treated by ammonia plasma. *Japanese Journal of Applied Physics*, *47*(9), 7346–7348.

Linder, M., Kochanowski, N., Fanni, J., & Parmentier, M. (2005). Response surface optimisation of lipase-catalysed esterification of glycerol and n-3 polyunsaturated fatty acids from salmon oil. *Process Biochemistry*, *40*(1), 273–279.

Mazerolles, G., Mathieu, D., Phan-tan-luu, R., & Siouffi, A. M. (1989). Computer-assisted optimization with nemrod software. *Journal of Chromatography A*, *485*, 433–451.

Mirajkar, R. N., Jamadar, S. A., Patil, A. V., & Mirajkar, N. S. (2011). Omega 3 fatty acids – Clinical implications. *International Journal of ChemTech Research*, *3*(2), 724–732.

Moisan, M., Beaudry, C., & Lepprince, P. (1974). A new HF device for the production of long plasma columns at a high electron density. *Physics Letters A*, *50*(2), 125–126.

Morra, M., Occhiello, E., & Garbassi, F. (1989). Contact angle hysteresis on oxygen plasma treated polypropylene surfaces. *Journal of Colloid and Interface Science*, *132*(2), 504–508.

Moser, E. M., Gilliéron, D., & Henrion, G. (2010). Durable anti-fogging effect and adhesion improvement on polymer surfaces. *The European Physical Journal: Applied Physics*, *49*, 1311–1312.

Mozafari, M. R. (2005). Liposomes: An overview of manufacturing techniques. *Cellular and Molecular Biology Letters*, *10*(4), 711–719.

Muzzarelli, R. A. A., Greco, F., Busilacchi, A., Sollazzo, V., & Gigante, A. (2012). Chitosan, hyaluronan and chondroitin sulfate in tissue engineering for cartilage regeneration: A review. *Carbohydrate Polymers*, *89*, 723–739.

Nirmala, R., Park, H.-M., Navamathavan, R., Kang, H.-S., El-Newehy, M. H., & Kim, H. Y. (2011). Lecithin blended polyamide-6 high aspect ratio nanofiber scaffolds via electrospinning for human osteoblast cell culture. *Materials Science and Engineering C*, *31*(2), 486–493.

Ogino, A., Kral, M., Yamashita, M., & Nagatsu, M. (2008). Effects of low-temperature surface-wave plasma treatment with various gases on surface modification of chitosan. *Applied Surface Science*, *255*(5, Part 1), 2347–2352.

Prabaharan, M., & Jayakumar, R. (2009). Chitosan-graft-β-cyclodextrin scaffolds with controlled drug release capability for tissue engineering applications. *International Journal of Biological Macromolecules*, *44*(4), 320–325.

Riaño, B., Molinuevo, B., & García-González, M. C. (2012). Optimization of chitosan flocculation for microalgal-bacterial biomass harvesting via response surface methodology. *Ecological Engineering*, *38*(1), 110–113.

Rotta, J., Ozório, R. Á., Kehrwald, A. M., de Oliveira Barra, G. M., de Melo Castanho Amboni, R. D., & Barreto, P. L. M. (2009). Parameters of color, transparency, water solubility, wettability and surface free energy of chitosan/hydroxypropylmethylcellulose (HPMC) films plasticized with sorbitol. *Materials Science and Engineering C*, *29*(2), 619–623.

Vesel, A., & Mozetic, M. (2012). Surface modification and ageing of PMMA polymer by oxygen plasma treatment. *Vacuum*, *86*(6), 634–637.

Wanichapichart, P., Sungkum, R., Taweepreda, W., & Nisoa, M. (2009). Characteristics of chitosan membranes modified by argon plasmas. *Surface and Coatings Technology*, *203*(17–18), 2531–2535.

Weska, R. F., Moura, J. M., Batista, L. M., Rizzi, J., & Pinto, L. A. A. (2007). Optimization of deacetylation in the production of chitosan from shrimp wastes: Use of response surface methodology. *Journal of Food Engineering*, *80*(3), 749–753.

Zhang, H. Y., Arab Tehrany, E., Kahn, C. J. F., Ponçot, M., Linder, M., & Cleymand, F. (2012). Effects of nanoliposomes based on soya, rapeseed and fish lecithins on chitosan thin films designed for tissue engineering. *Carbohydrate Polymers*, *88*(2), 618–627.

Zhao, X., Jiang, R., Zu, Y., Wang, Y., Zhao, Q., Zu, B., et al. (2012). Process optimization studies of 10-hydroxycamptothecin (HCPT)-loaded folate-conjugated chitosan nanoparticles by SAS-ionic crosslink combination using response surface methodology (RSM). *Applied Surface Science*, *258*(6), 2000–2005.